J. Astron. Space Sci. 14(2), 194–201 (1997)

NEAR-INFRARED PHOTOMETRY OF METAL RICH GLOBULAR CLUSTER M71

Jae-Mann Kyeong
Korea Astronomy Observatory, Daejeon 305-348, Korea
e-mail: jmkyeong@hanul.issa.re.kr

Yong-Ik Byun
Institute of Astronomy, National Central University, Chung-Li, Taiwan 32054, ROC
e-mail: byun@tien.phy.ncu.edu.tw

Mun-Suk Chun
Astronomy Program, Yonsei University, Seoul 120-749, Korea
e-mail: mschun@galaxy.yonsei.ac.kr

(Received October 31, 1997; Accepted November 20, 1997)

ABSTRACT

We have carried out JK near-infrared photometry for the central region of the metal rich globular cluster M71, whose $(K, J-K)$ color-magnitude diagram is presented here. Using two independent methods we derive the distance modulus to M71, 12.89 and 12.86 $\pm$ 0.12 respectively. The former is derived using the HB luminosity $M_{K_o}(HB) = -1.15$ for globular clusters having metallicity between -1.0 to -0.3 (Kuchinski *et al.* 1995). The latter is derived through a comparison with IR photometry of stars in the similar metallicity cluster 47 Tuc. We also estimate the reddening to M71, $E(J-K) = 0.13$, based on $E(B-V) = 0.04$ of 47 Tuc.

1. INTRODUCTION

An infrared study of giant stars in globular clusters has several advantages over optical approach. The effect of extinction is much reduced in IR; *i.e.* A_K=0.1A_V. The contrast between the redder cluster stars and bluer background and foreground stars are enhanced in the IR. Using these advantages and the large format IR arrays recently became available, we now have much better chance of making more extensive and systematic study on the properties of cluster giants. Kuchinski & Frogel (1995), for example, have successfully derived correlations among distance-independent and reddening-independent parameters for metal-rich system of disk clusters.

M71 (NGC6838, $l = 56.7°, b = -4.6°$) is a metal-rich globular cluster close to the galactic plane. Together with 47 Tuc it is one of the brightest and nearest of the disk globular clusters and can be studied more detaily. Because it is relatively close and only moderately reddended, M71 is an important comparison object for other metal-rich clusters. Field star contamination and differential

Table 1. Journal of Observations.

Date	Object	Location	Exposure	FWHM
	sky	30′ south	7x3sec(J)	
	M71	Center	7x3sec(J)	1.1″
July 29	sky	30′ south	7x3sec(J)	
1993	sky	30′ south	7x3sec(K′)	
	M71	Center	7x3sec(K′)	0.9″
	sky	30′ south	7x3sec(K′)	

reddening across the cluster, however, complicate detailed studies of cluster stars (Davidge & Simons 1994).

The effect of differential reddening however can be greatly reduced by observing clusters at wavelength longward of 1 micron. Frogel *et al.* (1979) was first to publish infrared photometry M71 and compared its giant branch morphology with a few other globular clusters and open cluster M67. However their aperture observations were limited to 25 giant and horizontal branch stars in the outer regions of the cluster .

In the present paper, we present J and K' imaging observations of the central region of M71. Details of our observations and reduction of the data are presented in Section 2. The photometric calibration of our data and (K, J-K) CMD are given in Section 3. Using our data and 47 Tuc IR data obtained by Frogel *et al.* (1981) we derive the distance modulus of M71 in Section 4. Section 5 summarizes our results.

2. OBSERVATION AND DATA REDUCTION

M71 was observed during the night of July 29 1993 using the University of Hawaii Infrared Camera (Hodapp *et al.* 1992), mounted at the Cassegrain focus of the UH 2.2m telescope. The camera contains a 256 × 256 HgCdTe NICMOS3 array with 40 micron pixels. The camera has two optical foci and our choice was the one which gives an image scale of 40.38″/pixel. Each image covered 1.6′. We used a jittering exposure scheme with 10″ offset between successive exposures in order to suppress bad pixels. The target field was observed through K' filter (Wainscoat & Cowie 1992) and Caltech-CTIO J filters. Besides the object frames, separate sky frames were obtained from a field 30′ south from the center of M71. For transformation to a standard system, 10 UKIRT faint standard stars were observed throughout three nights of our observing run which included other program objects. The detailed journal of observation is given in Table 1.

A median of dark frames recorded at the beginning and end of the night was substracted from all raw frames of the same exposure time. After linearization procedure, sky background images were constructed by median combining and were substracted from all object frames. The images were then divided by normalized flat frame, which was prepared by combining the difference between domeflat images of lamp-on and lamp-off. Experiments with several other options including the use

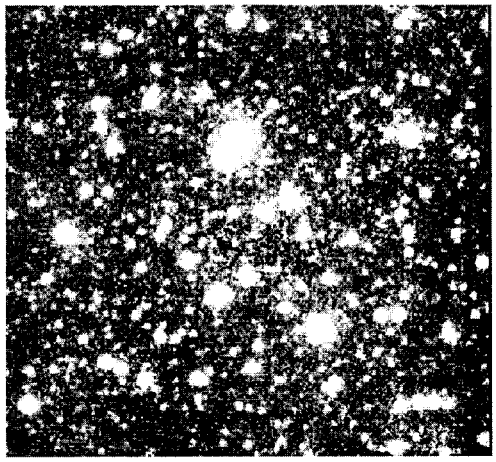

Figure 1. Final J image of the central region of M71. Individual exposure time was 3 seconds and 7 jitterred frames were combined by median filtering. North is to the left, east is to the top.

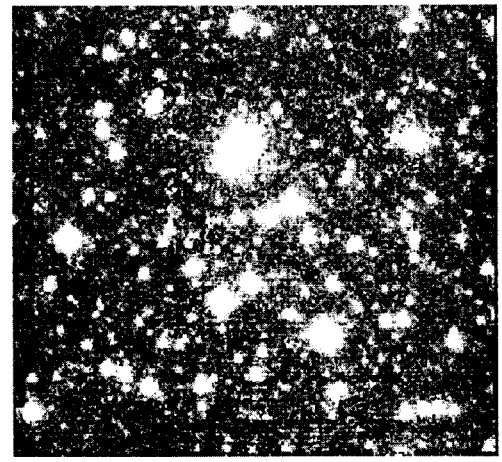

Figure 2. Final K' image of the central region of M71. Otherwise the same as Figure 1.

of sky flats proved that this method provides most stable and reliable results. Finally we combined each frame after shifting them for telescope offset of jittering observations. The final combined images are presented Figure 1 (J image) and 2 (K' image).

3. PHOTOMETRY AND COLOR-MAGNITUDE DIAGRAM

Stellar brightness were measured using the PSF fitting routine ALLSTAR, which is a part of IRAF/DAOPHOT photometry package (Stetson & Harris 1988). The photometry was calibrated based on aperture photometry of standard star frames. The zero points derived from these data have uncertainties about ± 0.03 magnitudes in J and K. And the color-term coefficients in the transformation equations were $-0.162(\pm 0.098)$ in J and $0.020(\pm 0.067)$ in K. For the extinction coefficient of Mauna Kea, we adopted the average value $k_J = 0.11$ and $k'_K = 0.06$ given by Guarnieri *et al.* (1991). After fixing the extinction coefficients at these values we made fits to the transformation relations to estimate color coefficients.

M71 is a relatively sparse cluster. The small areal coverage of the current observation, combined with the low stellar density, prevented us from obtaining photometry of a large number of cluster giants. Nevertheless our observation recovers the giant branch, horizontal branch and subgiant branch stars. Fully transformed J and K magnitudes for 262 stars are listed in Table 2 and the K vs. $J - K$ color magnitude diagram is presented in Figure 3.

Note that the bright end of the RGB is probably truncated because the brightest stars ($K < 7$) on the frame have been saturated and therefore excluded from our measurement. Frogel *et al.* (1979)

Table 2. J, K photometric data of 262 M71 stars.

ID	X	Y	J	σ_J	K	σ_K	ID	X	Y	J	σ_J	K	σ_K
1	148.06	199.65	10.286	0.058	9.389	0.067	61	276.98	226.62	14.131	0.040	13.574	0.038
2	144.88	126.88	10.388	0.032	9.467	0.032	62	111.24	246.52	14.141	0.034	13.761	0.048
3	63.91	159.94	10.421	0.020	9.456	0.038	63	269.26	159.37	14.178	0.033	13.615	0.040
4	245.04	211.75	10.431	0.031	9.656	0.030	64	45.17	87.08	14.220	0.041	13.481	0.037
5	181.96	177.52	10.861	0.047	9.889	0.036	65	110.98	235.34	14.236	0.033	13.592	0.036
6	44.71	69.25	11.113	0.048	10.368	0.044	66	187.97	131.87	14.265	0.049	13.761	0.038
7	160.10	136.61	11.162	0.035	10.383	0.051	67	100.88	116.18	14.291	0.027	13.583	0.036
8	154.77	272.77	11.221	0.027	10.422	0.036	68	242.30	126.90	14.298	0.034	13.500	0.031
9	133.84	82.96	11.978	0.024	11.214	0.026	69	270.62	216.35	14.320	0.038	13.696	0.033
10	109.31	229.77	11.993	0.047	11.131	0.032	70	98.24	153.53	14.389	0.032	13.769	0.033
11	105.89	82.40	12.060	0.041	11.251	0.045	71	273.36	200.55	14.444	0.032	14.081	0.056
12	129.52	144.90	12.078	0.042	11.151	0.031	72	133.82	72.40	14.456	0.050	13.982	0.056
13	230.23	116.24	12.287	0.040	11.797	0.037	73	253.54	239.04	14.514	0.043	13.882	0.041
14	265.82	106.02	12.353	0.046	11.664	0.038	74	197.01	188.71	14.548	0.041	14.057	0.048
15	82.66	216.50	12.366	0.040	11.731	0.044	75	256.31	210.43	14.556	0.035	14.173	0.050
16	84.58	91.95	12.383	0.044	11.635	0.034	76	180.39	184.38	14.611	0.048	13.976	0.072
17	189.73	159.87	12.402	0.032	11.721	0.028	77	279.94	116.50	14.612	0.047	14.115	0.069
18	89.14	205.50	12.415	0.037	11.745	0.034	78	135.15	271.12	14.617	0.042	13.911	0.039
19	250.51	69.88	12.416	0.047	11.838	0.026	79	177.80	49.76	14.657	0.032	14.007	0.061
20	214.70	156.86	12.421	0.028	11.894	0.038	80	233.04	228.94	14.691	0.108	14.565	0.099
21	33.56	218.13	12.436	0.057	13.411	0.225	81	160.03	47.96	14.707	0.033	14.410	0.098
22	256.99	36.45	12.442	0.089	12.686	0.283	82	126.83	156.45	14.711	0.032	14.178	0.050
23	202.69	135.81	12.470	0.022	11.862	0.025	83	123.12	232.34	14.719	0.039	14.137	0.040
24	239.32	116.72	12.492	0.045	11.837	0.036	84	57.71	87.69	14.739	0.029	14.056	0.047
25	85.99	256.61	12.493	0.033	11.877	0.034	85	128.78	118.49	14.753	0.039	14.260	0.056
26	205.97	80.25	12.493	0.041	11.995	0.042	86	80.84	175.70	14.795	0.037	14.563	0.067
27	93.40	88.57	12.495	0.034	11.874	0.041	87	163.36	158.45	14.839	0.035	14.252	0.055
28	258.04	70.51	12.509	0.038	11.864	0.039	88	152.66	97.14	14.859	0.038	14.130	0.046
29	240.41	68.27	12.510	0.043	11.827	0.030	89	259.44	255.33	14.874	0.050	14.623	0.064
30	162.46	88.46	12.532	0.034	11.802	0.047	90	193.57	209.47	14.876	0.059	14.406	0.058
31	283.78	143.88	12.533	0.044	12.177	0.075	91	242.65	177.32	14.888	0.043	14.366	0.055
32	80.88	227.69	12.637	0.053	11.778	0.036	92	216.43	122.66	14.920	0.065	14.702	0.087
33	242.18	270.41	12.681	0.033	11.982	0.024	93	211.92	198.54	14.924	0.077	14.298	0.082
34	95.45	264.55	12.730	0.027	11.905	0.025	94	223.43	152.16	14.960	0.058	14.291	0.061
35	170.85	170.57	12.768	0.047	12.013	0.035	95	221.05	51.31	14.991	0.043	14.258	0.050
36	166.22	171.83	12.987	0.046	12.200	0.033	96	103.50	261.87	15.025	0.024	14.238	0.046
37	74.93	182.79	13.055	0.032	12.305	0.040	97	239.98	261.57	15.032	0.032	14.528	0.058
38	153.26	170.55	13.105	0.039	12.404	0.021	98	187.60	108.50	15.067	0.097	14.463	0.122
39	180.65	120.22	13.122	0.058	12.361	0.054	99	60.06	111.99	15.070	0.050	14.463	0.062
40	54.22	135.67	13.126	0.032	12.180	0.026	100	203.34	76.90	15.095	0.127	14.012	0.117
41	113.90	105.31	13.136	0.029	12.462	0.033	101	229.30	133.26	15.116	0.059	14.761	0.071
42	263.46	42.57	13.164	0.123	13.544	0.186	102	246.18	281.85	15.133	0.052	14.366	0.068
43	244.71	160.44	13.182	0.033	12.358	0.036	103	158.84	191.62	15.140	0.070	14.257	0.049
44	168.19	268.62	13.217	0.026	12.498	0.036	104	281.19	244.95	15.169	0.041	14.763	0.068
45	117.18	163.94	13.229	0.042	12.568	0.040	105	144.82	112.42	15.240	0.063	14.652	0.053
46	235.36	212.84	13.362	0.026	12.817	0.037	106	192.64	269.24	15.247	0.106	14.672	0.108
47	209.31	190.81	13.456	0.046	12.692	0.043	107	140.12	86.92	15.267	0.046	14.621	0.062
48	104.04	141.60	13.484	0.036	12.866	0.034	108	198.91	159.36	15.269	0.055	14.642	0.069
49	173.33	227.51	13.504	0.042	13.011	0.051	109	125.08	107.08	15.278	0.047	14.578	0.074
50	165.44	100.27	13.528	0.040	12.727	0.044	110	109.78	271.33	15.290	0.040	14.526	0.049
51	253.53	180.79	13.545	0.029	12.943	0.031	111	47.02	176.37	15.292	0.067	14.555	0.061
52	283.46	50.30	13.620	0.037	12.903	0.056	112	78.12	120.32	15.335	0.045	14.689	0.062
53	244.79	149.40	13.697	0.032	13.406	0.033	113	280.27	201.44	15.346	0.054	15.111	0.076
54	86.04	181.83	13.779	0.030	12.994	0.044	114	248.46	51.51	15.373	0.062	14.686	0.070
55	113.73	158.09	13.787	0.031	12.996	0.029	115	240.18	236.97	15.380	0.112	15.077	0.110
56	245.54	275.57	13.895	0.034	13.236	0.043	116	273.60	131.08	15.388	0.054	15.347	0.107
57	73.31	104.00	13.978	0.042	13.235	0.037	117	170.43	140.52	15.389	0.059	14.958	0.102
58	265.63	69.43	14.049	0.075	13.343	0.072	118	234.83	107.71	15.396	0.055	15.025	0.106
59	122.26	104.12	14.056	0.028	13.331	0.034	119	218.30	95.48	15.400	0.053	15.218	0.083
60	49.22	215.41	14.114	0.032	13.463	0.037	120	68.26	192.34	15.420	0.057	15.053	0.084

Table 2. (continude).

ID	X	Y	J	σ_J	K	σ_K	ID	X	Y	J	σ_J	K	σ_K
121	125.42	261.17	15.464	0.045	14.998	0.073	181	74.02	201.19	15.907	0.079	15.091	0.082
122	176.20	140.51	15.466	0.079	15.197	0.104	182	59.83	279.34	15.907	0.087	15.297	0.115
123	204.89	104.25	15.473	0.096	14.619	0.103	183	238.42	282.84	15.917	0.078	15.196	0.099
124	207.99	117.63	15.510	0.058	14.945	0.117	184	146.85	48.92	15.921	0.049	15.083	0.089
125	209.58	231.33	15.513	0.095	14.897	0.095	185	187.62	262.85	15.923	0.075	15.051	0.099
126	203.74	205.42	15.528	0.046	15.072	0.095	186	179.29	219.46	15.924	0.063	15.346	0.095
127	131.52	106.66	15.529	0.055	15.157	0.083	187	94.42	244.43	15.931	0.107	15.717	0.155
128	217.26	187.70	15.531	0.062	15.034	0.082	188	85.54	229.49	15.933	0.100	14.960	0.105
129	228.46	235.60	15.542	0.056	15.702	0.116	189	194.55	146.34	15.934	0.110	15.625	0.143
130	173.28	176.07	15.544	0.071	14.997	0.152	190	190.56	152.57	15.938	0.075	15.465	0.120
131	153.57	154.30	15.550	0.046	15.119	0.089	191	179.31	103.58	15.938	0.080	15.483	0.109
132	200.26	261.47	15.584	0.069	14.870	0.078	192	70.14	149.66	15.940	0.071	15.378	0.091
133	262.54	236.28	15.588	0.067	15.219	0.130	193	109.47	255.77	15.958	0.065	15.538	0.121
134	216.92	224.23	15.599	0.092	15.008	0.088	194	269.86	260.36	15.960	0.085	15.345	0.126
135	124.37	213.62	15.607	0.057	14.930	0.087	195	201.84	66.69	15.970	0.078	15.148	0.138
136	171.32	197.47	15.614	0.078	15.130	0.085	196	141.98	153.66	15.971	0.100	15.192	0.088
137	228.46	235.60	15.629	0.056	15.249	0.094	197	242.35	102.08	15.982	0.085	15.514	0.116
138	35.29	168.87	15.641	0.119	14.738	0.130	198	60.95	61.35	15.983	0.057	15.272	0.107
139	184.38	214.25	15.643	0.066	15.228	0.096	199	285.40	81.28	15.996	0.089	15.618	0.108
140	117.10	133.76	15.648	0.078	15.440	0.110	200	143.87	225.33	16.004	0.063	15.633	0.148
141	248.18	239.22	15.660	0.086	15.270	0.102	201	270.75	165.70	16.005	0.065	15.430	0.113
142	80.91	124.20	15.661	0.100	15.073	0.079	202	183.43	283.99	16.008	0.063	15.324	0.108
143	165.22	217.35	15.670	0.147	14.838	0.122	203	86.18	109.50	16.009	0.083	15.427	0.115
144	94.21	81.35	15.674	0.049	14.982	0.058	204	262.46	51.70	16.020	0.083	15.420	0.114
145	175.91	81.75	15.689	0.111	15.136	0.141	205	267.46	131.23	16.021	0.106	15.678	0.147
146	142.29	169.19	15.692	0.066	15.065	0.113	206	167.50	65.96	16.023	0.105	15.317	0.131
147	226.61	233.31	15.699	0.071	15.702	0.116	207	181.71	204.98	16.024	0.067	15.837	0.171
148	276.30	249.72	15.700	0.057	15.013	0.090	208	267.05	208.22	16.028	0.073	15.388	0.117
149	222.55	83.02	15.712	0.053	15.695	0.154	209	76.77	155.90	16.040	0.087	15.369	0.116
150	142.79	179.72	15.721	0.055	15.362	0.099	210	149.03	223.78	16.047	0.098	15.231	0.098
151	267.67	141.11	15.723	0.070	14.959	0.078	211	135.76	153.51	16.063	0.131	15.612	0.179
152	130.43	136.26	15.733	0.079	14.961	0.080	212	161.52	222.77	16.064	0.100	15.439	0.117
153	166.41	108.91	15.744	0.086	15.420	0.122	213	214.27	220.28	16.068	0.068	15.444	0.116
154	119.39	274.01	15.745	0.052	15.052	0.078	214	278.97	126.05	16.071	0.092	15.403	0.127
155	106.55	110.55	15.750	0.059	15.336	0.120	215	54.28	100.43	16.072	0.092	15.779	0.196
156	86.63	105.68	15.759	0.081	15.326	0.111	216	65.02	83.42	16.084	0.090	15.520	0.127
157	205.22	163.64	15.759	0.070	15.582	0.137	217	285.04	283.64	16.085	0.064	15.131	0.095
158	125.38	193.02	15.772	0.060	15.434	0.098	218	201.10	223.62	16.107	0.091	15.807	0.207
159	138.16	169.21	15.773	0.083	15.441	0.159	219	201.95	254.25	16.120	0.083	15.685	0.135
160	118.46	215.28	15.774	0.092	15.413	0.113	220	219.68	215.38	16.132	0.125	15.504	0.122
161	65.21	128.59	15.774	0.053	15.307	0.112	221	39.95	246.14	16.139	0.081	15.544	0.106
162	74.51	258.73	15.776	0.113	15.056	0.115	222	116.68	175.10	16.143	0.107	15.524	0.175
163	128.20	161.47	15.793	0.058	15.418	0.098	223	172.46	251.25	16.181	0.078	15.641	0.116
164	73.36	91.32	15.794	0.072	15.464	0.118	224	154.57	228.52	16.183	0.080	15.098	0.125
165	215.03	216.34	15.800	0.070	15.216	0.104	225	201.15	179.70	16.188	0.081	15.730	0.156
166	237.23	174.72	15.801	0.059	15.399	0.114	226	123.03	239.91	16.201	0.080	15.612	0.115
167	221.62	139.09	15.803	0.052	15.611	0.096	227	231.10	207.86	16.211	0.098	15.583	0.137
168	107.05	121.10	15.805	0.123	15.238	0.155	228	239.99	243.76	16.214	0.062	15.715	0.180
169	199.40	88.50	15.828	0.068	15.138	0.076	229	48.83	275.89	16.214	0.091	15.199	0.112
170	131.00	161.50	15.835	0.080	15.418	0.098	230	43.04	78.53	16.230	0.084	15.500	0.101
171	128.20	161.47	15.837	0.058	15.191	0.086	231	230.22	214.68	16.231	0.115	15.687	0.142
172	215.17	59.05	15.848	0.059	15.292	0.088	232	239.26	220.39	16.240	0.111	15.352	0.168
173	235.58	90.50	15.863	0.088	15.520	0.115	233	143.99	146.17	16.242	0.113	15.376	0.127
174	131.00	161.50	15.879	0.080	15.191	0.086	234	141.19	260.20	16.251	0.085	15.874	0.202
175	278.80	195.24	15.889	0.072	15.508	0.156	235	242.48	242.23	16.255	0.082	15.715	0.180
176	47.30	185.63	15.897	0.080	15.436	0.101	236	104.66	235.42	16.273	0.093	15.617	0.125
177	77.85	258.58	15.899	0.080	15.360	0.128	237	234.70	143.95	16.278	0.093	15.824	0.164
178	221.93	207.75	15.903	0.070	15.571	0.155	238	202.92	99.10	16.281	0.113	15.171	0.120
179	91.08	99.55	15.903	0.083	15.485	0.118	239	158.06	145.96	16.291	0.108	15.633	0.116
180	61.92	227.60	15.904	0.116	15.640	0.160	240	125.08	245.79	16.291	0.082	15.855	0.157

Table 2. (continude).

ID	X	Y	J	σ_J	K	σ_K	ID	X	Y	J	σ_J	K	σ_K
241	116.64	184.62	16.293	0.135	15.673	0.141	252	90.83	164.56	16.404	0.098	15.786	0.133
242	147.88	84.84	16.295	0.098	15.977	0.142	253	74.15	37.06	16.410	0.108	15.646	0.133
243	78.86	205.27	16.297	0.099	16.028	0.190	254	85.06	117.36	16.418	0.094	15.741	0.147
244	236.25	97.13	16.300	0.106	15.798	0.172	255	67.67	126.22	16.421	0.095	15.525	0.144
245	209.72	248.17	16.306	0.097	15.743	0.156	256	224.67	124.13	16.480	0.101	15.624	0.090
246	270.16	275.79	16.339	0.111	15.535	0.136	257	131.31	282.19	16.510	0.100	15.549	0.105
247	258.05	142.55	16.342	0.083	15.715	0.117	258	47.39	120.79	16.523	0.108	15.516	0.122
248	137.44	195.51	16.353	0.113	15.537	0.152	259	163.34	112.65	16.544	0.128	16.175	0.231
249	58.60	238.40	16.359	0.083	15.713	0.150	260	172.86	77.25	16.560	0.113	15.803	0.144
250	114.94	278.08	16.370	0.137	15.340	0.086	261	60.53	103.33	16.622	0.139	15.845	0.154
251	135.76	253.57	16.385	0.091	15.736	0.130	262	33.73	86.12	16.650	0.088	15.750	0.127

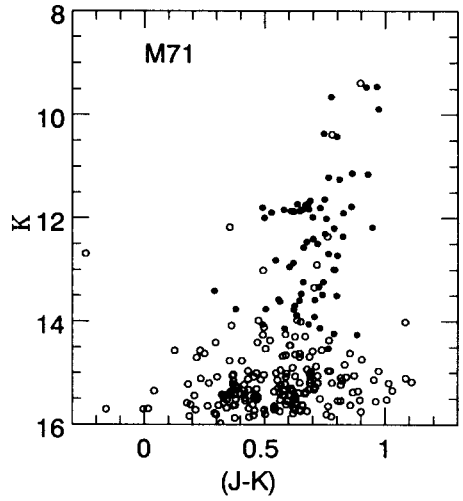

Figure 3. $(K, J-K)$ CMD of M71. The open circles represent the photometric error greater then 0.05, the filled circles less then 0.05.

reported a star as bright as 6.85 mag in K. Due to rarity of red giant stars and their large scatter, we cannot determine the slope of giant branch with any accuracy. This means that we cannot estimate the metallicity of M71 using the relation between [Fe/H] and $(J-K)_{GB}$ slope.

4. DISTANCE

According to many studies available for M71, the reddening value of M71 was determined well compared with the other globular clusters. Most study agree to the value of $E(B-V) = 0.28$ with small dispersion (Richer & Fahlman 1989). Based on this value, we derive the distance to M71 as following.

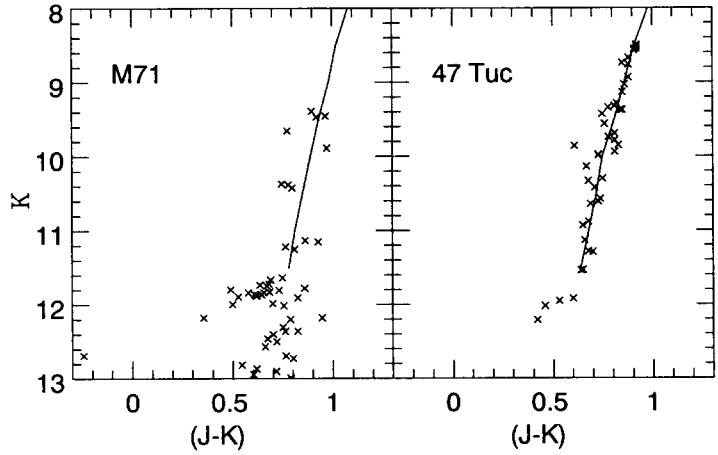

Figure 4. The mean locus of giant branch for M71 (left) and 47 Tuc (right). 47 Tuc data were taken from Frogel *et al.* (1981).

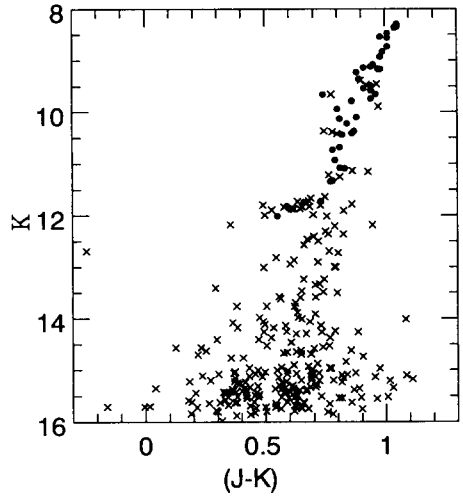

Figure 5. The data of M71 (cross) are overlaped to 47 Tuc stars (filled circle) shifted in both axes of CMD.

The absolute magnitude of the HB, $M_{K_o}(HB)$, is required for driving distances to clusters for which primarily near-IR data are available. Also, this parameter appears to have little or no sensitivity to a cluster's [Fe/H]. Kuchinski *et al.* (1995) estimates $M_{K_o}(HB) = -1.15 \pm 0.1$ based on 4 metal rich globular clusters. We obtained $K(HB) = 11.84$ from our CMD. From $E(B-V) = 0.28$ and the above result, we derive the distance modulus of M71 as 12.89.

We also use another method to estimate the distance to M71 using JK photometry of 47 Tuc

stars published by Frogel *et al.* (1981). We determined the horizontal and vertical offsets needed to bring the 47 Tuc data into an overlap with our M71 observations. This process is shown in Figure 4 and Figure 5. The offsets for the displayed match are $\Delta(m-M)_K = -0.20 \pm 0.05$ and $\Delta(J-K) = 0.13 \pm 0.05$, where the error indicates a reasonable range for acceptable fits. It seems that the match between the two clusters is rather good, supporting the metallicity of the two clusters are similar. In matching two data sets, we made efforts to overlap HB stars and the red giant branch stars. We then adopt following parameters for 47 Tuc, $E(B-V) = 0.04$ and $(m-M) = 13.14$ (Lee 1977), and the reddening raw $A_V = 3.12E(B-V), E(J-K) = 0.56E(B-V)$ (Bessell & Brett 1988). From the offsets discussed above, we find $E(J-K) = 0.13$ for M71 and the distance modulus as $(m-M)_{M71} = (m-M)_{47\,Tuc} + 0.624\Delta(J-K)$. We therefore get the distance modulus of 12.86 ± 0.12.

5. SUMMARY

We presented J and K photometric data and CMD $(K, J-K)$ of the central region of M71. And we derived its distance modulus using two independent methods. Based on $M_{Ko} = -1.15$ for metal rich globular cluster (Kuchinski *et al.* 1995), we determined the distance modulus as 12.89. In the other approach, the CMD data of 47 Tuc having well determined distance modulus were shifted to our data in both luminosity and color axes considering the reddening difference. From this, we derived the distance modulus of M71 as 12.86 ± 0.12 and $E(J-K) = 0.13$. The two estimates agree each other very well.

ACKNOWLEDGEMENTS: We would like to thank the support staffs at Univ. of Hawaii for their assistance during our observing run. YIB was supported by the National Science Council of the Republic of China through the grant NSC87-2112-M-008-025.

REFERENCE

Bessell, M. S. & Brett, J. M. 1988, PASP, 100, 1134
Davidge, T. J. & Simons, D. A. 1994, ApJ, 435, 207
Frogel, J. A., Persson, S. E. & Cohen, J. G. 1979, ApJ, 227, 499
Frogel, J. A., Persson, S. E. & Cohen, J. G. 1981, ApJ, 246, 842
Guarnieri, M. D., Dixon, R. L. & Longmore, A. J. 1991, PASP, 103, 675
Hodapp, K.-W., Rayner, J. & Irwin, E. 1992, PASP, 104, 441
Kuchinski, L. E. & Frogel, J. A. 1995, AJ, 110, 2844
Kuchinski, L. E., Frogel, J. A., Terndrup, D. M. & Persson, S. E. 1995, AJ, 109, 1131
Lee, S.-W. 1977, A&Ap Suppl., 27, 381
Richer, H. B. & Fahlman, G. G. 1989, ApJ, 339, 178
Stetson, P. B. & Harris, W. E. 1988, AJ, 96, 909
Wainscoat, R. J. & Cowie, L. L. 1992, AJ, 103, 332